

# Sensitivity of an optical feedback interferometer for acoustic waves measurements

Simon Chanu–Rigaldies,<sup>1,a)</sup>  Pierre Lecomte,<sup>2</sup> Sébastien Ollivier,<sup>2</sup> and Thomas Castelain<sup>2</sup> 

<sup>1</sup>Université de Lyon, Ecole Centrale de Lyon, Centre National de la Recherche Scientifique, Université Claude Bernard Lyon 1, Institut National des Sciences Appliquées de Lyon, Laboratoire de Mécanique des Fluides et d'Acoustique, Unité Mixte de Recherche 5509, 69130 Ecully, France

<sup>2</sup>Université de Lyon, Université Claude Bernard Lyon 1, Centre National de la Recherche Scientifique, Ecole Centrale de Lyon, Institut National des Sciences Appliquées de Lyon, Laboratoire de Mécanique des Fluides et d'Acoustique, Unité Mixte de Recherche 5509, 69622 Villeurbanne, France

[simon.chanu-rigaldies@ec-lyon.fr](mailto:simon.chanu-rigaldies@ec-lyon.fr), [pierre.lecomte@univ-lyon1.fr](mailto:pierre.lecomte@univ-lyon1.fr), [sebastien.ollivier@univ-lyon1.fr](mailto:sebastien.ollivier@univ-lyon1.fr), [thomas.castelain@univ-lyon1.fr](mailto:thomas.castelain@univ-lyon1.fr)

**Abstract:** This work presents a sensitivity study on the use of an optical feedback interferometer to measure acoustic pressure from plane waves. The sensitivity is established by linearising the interferometer's governing equations. It is shown to be independent of the acoustic wave frequency but dependent on configuration parameters such as the optical feedback parameter or the length of the laser through which the acoustic wave passes. Experimental validation is carried out using three acoustic waveguides in the 0.5–18 kHz range. The sensitivity obtained enables broadband acoustic pressure measure with a low mean relative error in comparison with a reference condenser microphone. © 2023 Author(s). All article content, except where otherwise noted, is licensed under a Creative Commons Attribution (CC BY) license (<http://creativecommons.org/licenses/by/4.0/>).

[Editor: Longjun Dong]

<https://doi.org/10.1121/10.0021317>

Received: 1 June 2023 Accepted: 23 September 2023 Published Online: 11 October 2023

## 1. Introduction

Acousto-optic methods for the detection and the characterization of acoustic waves have been extensively developed and studied.<sup>1–4</sup> They rely on the interferometric measurement of optical index variation caused by the acoustic waves: the acousto-optic effect. Recently, an optical feedback interferometer (OFI), also referred as a self-mixing interferometer, has been proposed for acoustic pressure field visualization.<sup>5,6</sup> This interferometric technique relies on the use of a semiconductor laser that is sensitive to light feedback effects. Indeed, if a fraction of the light emitted by a laser diode returns in its cavity by reflection or scattering, its behavior changes in terms of emitted power and optical wavelength according to the optical path followed by the laser beam.<sup>7</sup> In practice, it is implemented by using a laser diode which targets a retro-reflective surface and interferences are measured with an embedded photodiode. Thus, the OFI has the advantage of requiring little equipment and being self-aligned compared to other types of interferometers. As well as other optical methods, the OFI performs an integrated measurement along the laser path. Therefore, knowledge of the radiation from the acoustic source is required to solve this integral.<sup>2,3</sup> Only a few studies have been conducted on the performance of the OFI for quantitative acoustic pressure measurement. In addition, the detection specifications in terms of amplitude, signal-to-noise ratio, and frequency content of the acoustic source are not clearly established for acoustic measurement with an OFI. Knudsen *et al.* studied the lower detection limit for 3 kHz plane sinusoidal waves in a waveguide and observed a proportionality between the OFI output signal and the sound pressure amplitude.<sup>8</sup> However, in the laser self-mixing theory<sup>7</sup> this proportionality is not highlighted by the equations and remains to be established. Also, the OFI sensitivity is supposed to be independent of the acoustic wave frequency, which is to be measured.

The purpose of this study is to characterize the sensitivity of the OFI to the acoustic pressure in a waveguide. A model of the OFI sensitivity for the measurement of acoustic plane waves is established. Measurements in acoustic waveguides validate this model. The paper is organized as follows: the equations that model the optical feedback and the response of an OFI to plane acoustic waves are detailed in Sec. 2. Then, the experimental apparatus is described in Sec. 3, it aims at measuring plane waves with an OFI and a microphone. The results are presented and discussed in Sec. 4. Finally, the conclusion and future works are described in Sec. 5.

<sup>a)</sup> Author to whom correspondence should be addressed.

## 2. OFI sensitivity to acoustic plane waves

In this section, a proportionality relationship is established between the acoustic pressure of a plane wave and the output signal of an OFI.

### 2.1 Acousto-optic effect

When an acoustic wave propagates through the air, the variation of acoustic pressure induces a local variation of the refractive index. The pressure  $p(\mathbf{r}, t)$ , at a given time  $t$  and position  $\mathbf{r}$  can be written as

$$p(\mathbf{r}, t) = p_0 + p'(\mathbf{r}, t), \quad (1)$$

where  $p_0$  is the mean pressure of the air and  $p'(\mathbf{r}, t)$  is the acoustic pressure. Similarly, the optical refractive index  $n(\mathbf{r}, t)$  can be written as follows:

$$n(\mathbf{r}, t) = n_0 + n'(\mathbf{r}, t), \quad (2)$$

where  $n_0$  is the mean refractive index and  $n'(\mathbf{r}, t)$  is the fluctuation of refractive index caused by the acoustic waves which is called the acousto-optic effect. The latter can be calculated using Ciddor's model<sup>9</sup> as proportional to the acoustic pressure,

$$n'(\mathbf{r}, t) = \beta(\lambda_0, p_0, T_0, \phi_h, c_{\text{CO}_2})p'(\mathbf{r}, t). \quad (3)$$

In Eq. (3),  $\beta$  is a quantity depending on:  $\lambda_0$  the electromagnetic wavelength,  $p_0$  the static pressure,  $T_0$  the temperature of the air,  $\phi_h$  the humidity rate, and  $c_{\text{CO}_2}$  the molar concentration of  $\text{CO}_2$ . It is then possible to calculate the acoustic pressure by measuring the refractive index of the medium by using an optical interferometer and Eq. (3). For laboratory conditions of  $\lambda_0 = 1309$  nm,  $p_0 = 1$  bar,  $T_0 = 20^\circ\text{C}$ ,  $\phi_h = 0.5$ , and  $c_{\text{CO}_2} = 440$  ppm, the value of  $\beta$  is  $2.6 \times 10^{-9} \text{ Pa}^{-1}$ .

As a laser beam goes through the medium in which acoustic waves propagate and reflects back from a surface into the laser cavity, the optical path  $\mathcal{L}$  along the beam is altered due to changes in the optical index of the medium. Thus, the optical path  $\mathcal{L}$  is expressed as follows:

$$\mathcal{L}(t) = 2 \int_0^{L(t)} n(x, t) dx, \quad (4)$$

where  $x$  is the coordinate along the laser beam,  $n(x, t)$  is the optical index at position  $x$ , and  $L(t)$  is the distance between the laser cavity and the reflecting surface. The latter is defined as  $L(t) = L_0 + L_V(t)$ , where  $L_0$  is the laser beam length at rest and  $L_V(t)$  is the geometric length variation of the laser beam due to possible displacements of the reflecting surface. It is assumed that the laser beam is not deflected. By combining Eqs. (2), (3), and (4), the optical path  $\mathcal{L}$  is rewritten as

$$\mathcal{L}(t) = 2 \left( n_0 L(t) + \beta \int_0^{L(t)} p'(x, t) dx \right) = 2n_0(L_0 + L_V(t) + L_{\text{AO}}(t)). \quad (5)$$

In Eq. (5),  $L_{\text{AO}}(t)$  is the apparent length variation of the laser beam caused by the acousto-optic effect.<sup>8</sup> For the sake of simplicity, the time variable  $t$  is dropped in the remaining equations.

### 2.2 Modeling the response of an OFI to acoustic plane waves

An OFI uses the self-mixing properties of laser diodes: if a fraction of the photons emitted by the laser diode returns into the laser cavity, the laser diode power and wavelength vary.<sup>7</sup> This phenomenon is known as optical feedback effect. If the amount of photons returning to the laser cavity is much smaller than the amount leaving it, which in practice can be obtained when the laser beam is backscattered from rough surfaces,<sup>10</sup> this phenomenon can be modeled as<sup>7</sup>

$$\frac{2\pi}{\lambda_0} \mathcal{L} = \frac{2\pi}{\lambda} \mathcal{L} + C \sin \left( \frac{2\pi}{\lambda} \mathcal{L} + \arctan(\alpha) \right). \quad (6)$$

In Eq. (6),  $\mathcal{L}$  is the optical path outside the laser's cavity,  $\lambda_0$  is the wavelength of the laser diode without optical feedback,  $\lambda$  is the actual wavelength of the laser with feedback,  $C$  is the feedback parameter that depends on the amount of light reflected back into the laser cavity, and  $\alpha$  is the linewidth enhancement factor.<sup>11</sup>

In the case where  $L_V$  is negligible with respect to  $L_{\text{AO}}$  in Eq. (5) and based on numerical simulations of Eq. (6),<sup>10</sup> the wavelength  $\lambda$  can be described as

$$\lambda = \lambda_{L_0} + \gamma L_{\text{AO}}, \quad (7)$$

where  $\lambda_{L_0}$  is the value of  $\lambda$  where  $L = L_0$  and  $\gamma$  is a coefficient depending on  $C$  and  $\alpha$ . Note that  $\lambda_{L_0} \gg \gamma L_{\text{AO}}$  for acoustic measurements which in practice means that the variation of the optical wavelength caused by  $L_{\text{AO}}$  is negligible compared to the value of  $\lambda_{L_0}$ .

The effect of the optical feedback on the laser power is modeled by the equation<sup>12</sup>

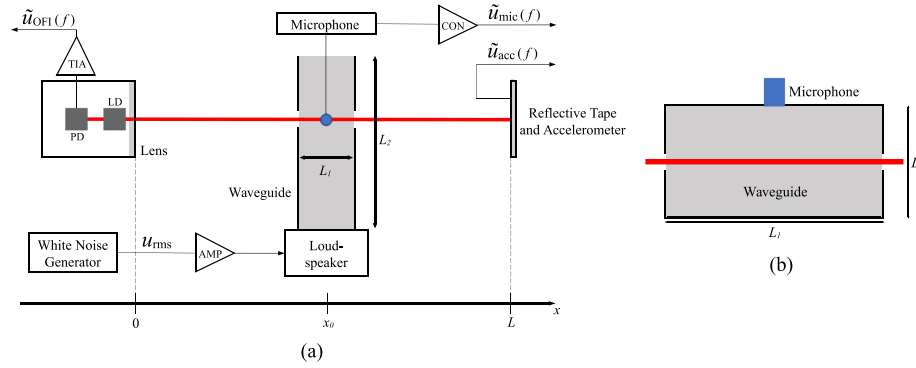


Fig. 1. (a) Scheme of the experimental setup. The OFI laser beam emitted by the laser diode (LD) crosses a section of the acoustic waveguide and points at the reflective tape. AMP is the power amplifier of the signal emitted by the white noise generator. CON is the microphone conditioner. TIA is the transimpedance amplifier that converts the current from the photodiode (PD) into a voltage which is the OFI signal. (b) Scheme of the waveguide section crossed by the laser beam.

$$\mathcal{P} = \mathcal{P}_0 \left( 1 + m \cos \left( \frac{2\pi}{\lambda} \mathcal{L} \right) \right), \tag{8}$$

where  $\mathcal{P}$  is the power of the laser diode,  $\mathcal{P}_0$  is the power of the laser diode without optical feedback, and  $m$  is the modulation index which is proportional to  $C$ . In a practical setup, the power of the laser diode  $\mathcal{P}$  is measured by using an embedded photodiode. Its current is converted into voltage by using a transimpedance amplifier, resulting in the OFI signal. One denotes  $u_{\text{OFI}}$  the alternative component (AC) of this signal.

For sinusoidal plane waves, it has been observed experimentally that  $u_{\text{OFI}}$  is proportional to  $L_{\text{AO}}$ .<sup>8</sup> However, there is no proportionality between  $\mathcal{P}$  and  $L_{\text{AO}}$  when replacing  $\mathcal{L}$  and  $\lambda$  in Eq. (8) by their expressions in Eqs. (5) and (7), respectively. Nevertheless, as detailed in the supplementary material one can obtain a proportional relationship under the following assumptions:

- (i)  $\cos(4\pi n_0 L_{\text{AO}}/\lambda) \simeq 1$ , which can be satisfied if  $L_{\text{AO}} \ll \lambda$ .
- (ii)  $\cos(4\pi n_0 L_0 \gamma L_{\text{AO}}/(\lambda_{L_0})^2) \simeq 1$ , which can be satisfied if  $L_{\text{AO}} \ll (\lambda_{L_0})^2/(L_0 \gamma)$ .

Using a first order Taylor series expansion, the relationship between  $u_{\text{OFI}}$  and  $L_{\text{AO}}$  is expressed as

$$u_{\text{OFI}} \simeq \frac{U_0 m 4\pi n_0}{\lambda_{L_0}} \left( \frac{L_0 \gamma}{\lambda_{L_0}} - 1 \right) \sin \left( \frac{4L_0 n_0 \pi}{\lambda_{L_0}} \right) L_{\text{AO}}, \tag{9}$$

where  $U_0$  is the direct component (DC) component of the OFI signal without optical feedback.

When an acoustic plane wave propagates perpendicularly to the laser beam, the latter lies along a wavefront whose pressure is constant.  $L_{\text{AO}}$  can then be described as

$$L_{\text{AO}} = \frac{\beta}{n_0} \int_0^L \Pi \left( \frac{x - x_0}{2L_1} \right) p' dx = \frac{\beta L_1}{n_0} p', \tag{10}$$

where  $\Pi$  is the rectangular function,  $p'$  is the acoustic pressure of the plane wave along the laser beam,  $L_1$  is the part of the laser beam that is disturbed by the plane wave centered in  $x = x_0$ . Thus,  $u_{\text{OFI}}$  can be written as

$$u_{\text{OFI}} = \kappa_{\text{OFI}} p', \tag{11}$$

where the OFI sensitivity  $\kappa_{\text{OFI}}$  (in V/Pa) is

$$\kappa_{\text{OFI}} \simeq \frac{U_0 m 4\pi n_0}{\lambda_{L_0}} \left( \frac{L_0 \gamma}{\lambda_{L_0}} - 1 \right) \sin \left( \frac{4L_0 n_0 \pi}{\lambda_{L_0}} \right) \frac{\beta L_1}{n_0}. \tag{12}$$

According to this formula, the sensitivity of the OFI depends on  $L_1$  but not on the frequency of the acoustic waves.

Table 1. Properties of the waveguides. See Fig. 1 for the nomenclature of the waveguide dimensions.

Waveguide No.	Dimensions $L_1 \times L_2 \times L_3$ (mm)	Waveguide end	TCOF (Hz)
1	45 × 430 × 25	Closed	3 500
2	35 × 350 × 35	Open	4 000
3	10 × 200 × 10	Open	18 000

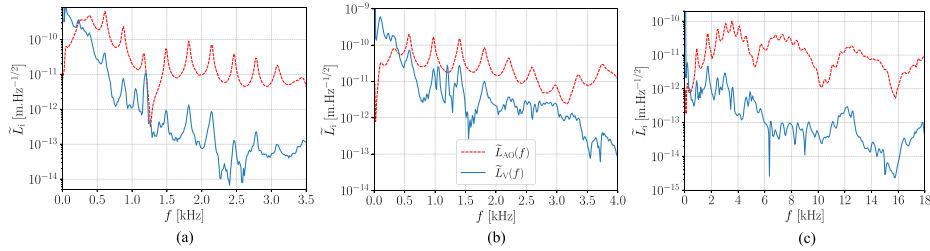


Fig. 2. Measurements of  $\tilde{L}_V(f)$  (in solid blue) and  $\tilde{L}_{AO}(f)$  (in dashed red) for (a) waveguide No. 1, (b) waveguide No. 2, and (c) waveguide No. 3 below their TCOF.  $u_{RMS} = 0.5$  V.

### 3. Experiments

The aim here is to capture acoustic waves in a section of a waveguide using a microphone and an OFI. One compares these two measurements to verify a proportionality relationship by linear regression and deduce  $\kappa_{OFI}$ . A scheme of the setup is shown in Fig. 1.

#### 3.1 The optical feedback interferometer

The laser diode (LD) of the OFI is a Thorlabs<sup>®</sup> L1310P5DFB with a maximum power of 5 mW and a wavelength  $\lambda_0 = 1309$  nm. It is embedded with a photodiode (PD), which delivers a current that is proportional to the power  $\mathcal{P}(t)$  of LD. The beam is collimated using a Thorlabs<sup>®</sup> C110TMD-C lens with a focal length of 6.24 mm. The LD is powered by a current driver Thorlabs<sup>®</sup> LDC205C and maintained at a constant temperature of 12 °C using a Thorlabs<sup>®</sup> TED200C temperature controller. The current from the PD is converted into a voltage  $u_{OFI}(t)$  with a transimpedance amplifier Femto<sup>®</sup> DLPCA-200 whose gain is set to  $10^4$  V/A.

The laser light spot of the OFI is positioned on a rough reflective tape placed at  $L_0 \simeq 40$  cm from the LD. It allows the return of a certain quantity of photons in its cavity by backscattering so that Eq. (6) is valid.<sup>10</sup> The reflective tape is glued on an accelerometer PCBpiezotronics<sup>®</sup> 352C65 linked to a PCBpiezotronics<sup>®</sup> 482C05 conditioner which delivers a voltage  $u_{acc}(t)$  that is proportional to the sensor acceleration. It allows the measurement of mechanical vibrations  $L_V(t)$  in Eq. (5).

The OFI feedback parameter  $C$  is adjusted by modifying the LD current. This parameter is related to the amount of light backscattered into the laser.<sup>7</sup> It strongly depends on the alignment of the laser beam and  $L_0$ . Adjusting the current, and thus the light intensity emitted by the laser diode, allows a finer and more controllable adjustment of the  $C$  parameter without changing the optical setup of the OFI.

#### 3.2 The acoustic waveguides

Three rectangular section acoustic waveguides were used in the frequency range below their theoretical cut-off frequency (TCOF) to satisfy the plane wave hypothesis that was assumed in Eq. (10).<sup>13</sup> The dimensions and acoustic properties of the waveguides are given in Table 1 with  $TCOF = c_0/(2L_1)$  ( $c_0$  is the speed of sound). The laser beam passes through the guide by two side holes. A reference microphone is flush-mounted above the beam in order to measure the acoustic pressure in the same section [see Fig. 1(b)]. The reference microphone is a 1/4" GRAS<sup>®</sup> 40BH (waveguides Nos. 1 and 2) or a 1/8" GRAS<sup>®</sup> 40DP (waveguide No. 3) connected to a Brüel & Kjaer<sup>®</sup> NEXUS 2690-A-0F2 conditioner. The latter delivers a voltage  $u_{mic}(t)$  proportional to the acoustic pressure  $p'(t)$  of the section. Each waveguide is excited by a different

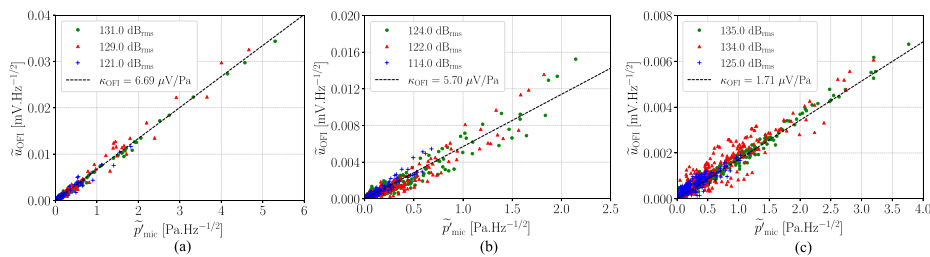


Fig. 3. ASD of the OFI signal  $\tilde{u}_{OFI}(f)$  as a function of  $\tilde{p}'_{mic}(f)$  in (a) waveguide No. 1, (b) waveguide No. 2, and (c) waveguide No. 3 for frequencies satisfying Eq. (15). Green circles are measurements made with  $u_{RMS} = 0.5$  V, red triangles with  $u_{RMS} = 0.3$  V, and blue crosses with  $u_{RMS} = 0.1$  V. The acoustic level (in dB<sub>RMS</sub>) of each measurement is given in the legend. The black dashed lines are linear regressions of slope  $\kappa_{OFI}$ .

Table 2. Measured sensibility and MRE for each waveguide with the maximum value of  $C$  for this setup.

Waveguide No.	1	2	3
$\kappa_{\text{OFI}}$ (V/Pa)	$6.69 \times 10^{-6}$	$5.71 \times 10^{-6}$	$1.71 \times 10^{-6}$
$\kappa_{\text{OFI}}/L_1$ [V/(Pa m)]	$1.48 \times 10^{-4}$	$1.63 \times 10^{-4}$	$1.71 \times 10^{-4}$
MRE (dB)	-6.5	-9.0	-4.6

loudspeaker at one of its extremities. They are powered by a Visaton<sup>®</sup> AMP 2.2 LN amplifier. Hereinafter, the “acoustic source” refers to the amplifier, loudspeaker, and waveguide assembly.

### 3.3 Measurement method

The excitation signal is a white noise generated in the range [0,20] kHz by a Siglab DSP 20–42 Dynamic Signal Analyzer controlled by a MATLAB program. The root mean square (RMS) value of the excitation signal is denoted  $u_{\text{RMS}}$ . For each waveguide, the acoustic waves are measured sequentially by the microphone and the OFI. For the latter, an additional background noise measurement, denotes  $u_{\text{noise}}(t)$ , is done with the loudspeaker turned off. Then, the amplitude spectral densities (ASD) are calculated by analyzing 1000 signal frames of 200 ms duration. One denotes  $\tilde{u}_{\text{mic}}(f)$ ,  $\tilde{u}_{\text{OFI}}(f)$ ,  $\tilde{u}_{\text{acc}}(f)$ , and  $\tilde{u}_{\text{noise}}(f)$  the ASD of  $u_{\text{mic}}(t)$ ,  $u_{\text{OFI}}(t)$ ,  $u_{\text{acc}}(t)$ , and  $u_{\text{noise}}(t)$ , respectively.

## 4. Results and discussion

The first step is to identify the frequency range in which the contribution of vibrations  $L_V$  can be neglected (Sec. 4.1). Then, the experimental method to estimate  $\kappa_{\text{OFI}}$  is detailed and the results are discussed (Sec. 4.2).

### 4.1 $L_V$ and $L_{\text{AO}}$ measurements

As the sensitivity of the OFI is not measured yet, it is not possible to separate the contributions of  $L_V$  and  $L_{\text{AO}}$  in the OFI signal [see Eqs. (5) and (8)]. However, they can be estimated from the ASDs of the accelerometer and the microphone voltage

$$\tilde{L}_V(f) = \frac{1}{4\pi^2 f^2 \kappa_{\text{acc}}} \tilde{u}_{\text{acc}}(f), \tag{13}$$

where  $\tilde{L}_V(f)$  is the ASD of  $L_V(t)$  and  $\kappa_{\text{acc}}$  is the sensitivity of the accelerometer [in V/(m/s<sup>2</sup>)] and

$$\tilde{L}_{\text{AO}}(f) = \frac{\beta L_1}{n_0} \frac{\tilde{u}_{\text{mic}}(f)}{\kappa_{\text{mic}}} = \frac{\beta L_1}{n_0} \tilde{p}'_{\text{mic}}(f), \tag{14}$$

where  $\tilde{L}_{\text{AO}}(f)$  is the ASD of  $L_{\text{AO}}(t)$ ,  $\tilde{p}'_{\text{mic}}(f) = \kappa_{\text{mic}} \tilde{u}_{\text{mic}}(f)$  is the estimated ASD of  $p'(t)$  by the microphone, and  $\kappa_{\text{mic}}$  is the proportionality coefficient between  $\tilde{u}_{\text{mic}}(f)$  and  $\tilde{p}'_{\text{mic}}(f)$  (in V/Pa). Note that Eq. (14) is only valid for plane waves. Measurements of  $\tilde{L}_V(f)$  and  $\tilde{L}_{\text{AO}}(f)$  for each waveguide are plotted in Fig. 2, showing their resonance frequencies.

Beyond 500 Hz for the waveguides Nos. 1 and 2, and 1 kHz for the waveguide No. 3,  $\tilde{L}_V(f)$  is for most frequencies at least 10 times lower than  $\tilde{L}_{\text{AO}}(f)$ . It allows one to consider that above these threshold frequencies,  $\tilde{L}_V(f)$  is negligible compared to  $\tilde{L}_{\text{AO}}(f)$  and that the variations in the OFI signal are mainly caused by the acoustic waves in the waveguide.

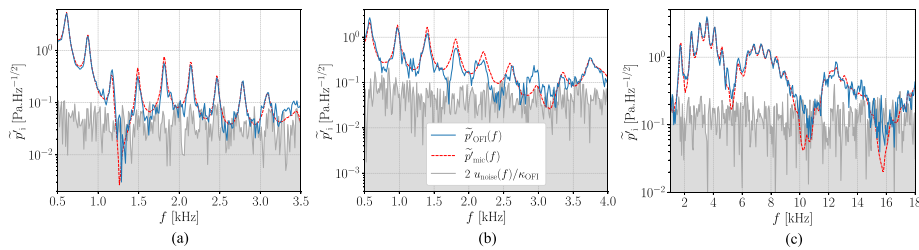


Fig. 4. Acoustic pressure estimated from the microphone  $\tilde{p}'_{\text{mic}}(f)$  (in dashed red) and the OFI  $\tilde{p}'_{\text{OFI}}(f)$  (in solid blue) as a function of the frequency of the acoustic waves for (a) waveguide No. 1, (b) waveguide No. 2, and (c) waveguide No. 3.  $\tilde{p}'_{\text{OFI}}(f)$  values which are not in the gray area are used for  $\kappa_{\text{OFI}}$  estimation.  $u_{\text{RMS}} = 0.5$  V.

Table 3. Measured sensibility for different values of  $C$  such as  $C_1 < C_2 < C_3$  on waveguide No. 1.

$C$	$C_1$	$C_2$	$C_3$
$\kappa_{\text{OFI}}$ (V/Pa)	$2.60 \times 10^{-6}$	$4.95 \times 10^{-6}$	$6.69 \times 10^{-6}$

#### 4.2 OFI sensitivity

Measurements are made for several excitation levels  $u_{\text{RMS}}$ , in order to have different values of  $\tilde{p}'_{\text{mic}}(f)$ . The OFI feedback parameter  $C$  is set to its maximum value for the experimental setup. In Fig. 3,  $\tilde{u}_{\text{OFI}}(f)$  is plotted as a function of  $\tilde{p}'_{\text{mic}}(f)$  for each frequency which respects

$$\begin{cases} \tilde{L}_{\text{AO}}(f) \geq 10 \tilde{L}_{\text{V}}(f), \\ f \leq \text{TCOF}, \\ \tilde{u}_{\text{OFI}}(f) \geq 2 \tilde{u}_{\text{noise}}(f). \end{cases} \quad (15)$$

The later condition, where the factor 2 is set arbitrarily, ensures that the points used for the linear regressions are sufficiently above the background noise  $\tilde{u}_{\text{noise}}(f)$ .<sup>8</sup> The OFI sensitivity is then estimated by performing a linear regression on the remaining data. According to Eq. (11), the slope of the linear regression is  $\kappa_{\text{OFI}}$  whose values for each waveguide are shown in Table 2. The linearization assumptions allowing the validity of Eq. (11) reach at least 0.94 for assumption (i) and 0.89 for assumption (ii).

Using these  $\kappa_{\text{OFI}}$  estimations, the acoustic pressure estimated by the OFI  $\tilde{p}'_{\text{OFI}}(f)$  is calculated by dividing  $\tilde{u}_{\text{OFI}}(f)$  by  $\kappa_{\text{OFI}}$ . Figure 4 compares the values of  $\tilde{p}'_{\text{mic}}(f)$  and  $\tilde{p}'_{\text{OFI}}(f)$  for each waveguide. Acoustic pressure estimations made with the microphone and the OFI are quite similar. For each waveguide, the mean relative error (MRE) over the  $N$  frequencies  $f_i$  which respect Eq. (15) is shown in Table 2. It is computed as follows:

$$\text{MRE} = \frac{1}{N} \sum_{f_i} \frac{|\tilde{p}'_{\text{mic}}(f_i) - \tilde{p}'_{\text{OFI}}(f_i)|}{\tilde{p}'_{\text{mic}}(f_i)}. \quad (16)$$

The low MRE values obtained suggest that  $\kappa_{\text{OFI}}$  is independent of the frequency. In addition, for the frequencies where  $\tilde{p}'_{\text{OFI}}(f)$  is getting closer to  $2 \tilde{u}_{\text{noise}}(f)/\kappa_{\text{OFI}}$  (the gray curves in Fig. 4), the similarity between  $\tilde{p}'_{\text{OFI}}(f)$  and  $\tilde{p}'_{\text{mic}}(f)$  decreases. Indeed,  $u_{\text{OFI}}$  may go below the lower detection limit.<sup>8</sup> It is therefore recommended to exclude these frequencies when estimating  $\kappa_{\text{OFI}}$ .

As  $\kappa_{\text{OFI}}$  is proportional to  $L_1$  [see Eq. (12)], values of  $\kappa_{\text{OFI}}/L_1$  are also calculated to remove the influence of the waveguide geometry on the OFI sensitivity and are presented in Table 2. It is observed that values of  $\kappa_{\text{OFI}}/L_1$  are of the same order of magnitude for each waveguide, which confirms a satisfactory  $\kappa_{\text{OFI}}$  estimation with this measurement method. Table 3 shows different  $\kappa_{\text{OFI}}$  values obtained for different values of  $C$ , set as explained in Sec. 3.1, with waveguide No. 1. These results show a reduction in the OFI sensitivity with the value of  $C$  as expected by Eq. (12). Differences between  $\kappa_{\text{OFI}}/L_1$  values of each waveguide may be due to the experimental method, or to the limit of validity of some hypotheses. In particular, the setting of the OFI-reflector path can be slightly modified when switching the waveguides, which can slightly change the values of  $C$  and  $\kappa_{\text{OFI}}$ . The validity of assumptions such as neglecting acoustic wave radiation from the waveguides side holes through which the optical beam passes would also require more attention in future studies to improve sensitivity estimation.

#### 5. Conclusion

A study of the optical feedback theory has demonstrated that the output signal of the OFI can be considered proportional to the acoustic pressure with two assumptions. The calculation of the sensitivity has shown that it does not depend on the frequency of the acoustic waves to be measured. The measurement of acoustic plane waves with a reference microphone and an OFI has allowed to calculate the sensitivity of the latter. The similarity between the OFI and the microphone acoustic pressure estimations in the range 0.5–18 kHz suggests an independence of the OFI sensitivity to the frequency. To verify this property on higher frequencies, it will be necessary to change the acoustic source. Future work includes the measurements of other acoustic sources to study the ability of the OFI to measure ultrasonic waves. To measure acoustic waves of larger amplitudes, the linearization assumptions can be defeated. Future work will present how to estimate  $p'$  from  $u_{\text{OFI}}$  beyond linearization conditions.

#### Supplementary Material

See the supplementary material for the linearization of Eq. (8).

## Acknowledgments

We thank Emmanuel Jondeau and Jean-Charles Vingiano for their help in the realization of the experimental setup and Edouard Salze for his readings. The present work is part of the program MAMBO “Méthodes Avancées pour la Modélisation du Bruit moteur et aviOn” (“Advanced methods for engine and aircraft noise modelling”) coordinated by Airbus SAS. It was supported by the Direction Générale de l’Aviation Civile (DGAC) under the Grant No. 2021–50. This work was supported by the Labex CeLyA of Université de Lyon, operated by the French National Research Agency (Grant No. ANR10-LABX-0060/ANR-11-IDEX-0007).

## Author Declarations

### Conflict of Interest

There are no conflicts of interest related to this work.

## Data Availability

The data that support the findings of this study are available from the corresponding author upon reasonable request.

## References

- <sup>1</sup>L. Zipsper and H. H. Franke, “Refracto-vibrometry—A novel method for visualizing sound waves in transparent media,” *J. Acoust. Soc. Am.* **123**(5), 3314 (2008).
- <sup>2</sup>P. Yuldashev, M. Karzova, V. Khokhlova, S. Ollivier, and P. Blanc-Benon, “Mach-Zehnder interferometry method for acoustic shock wave measurements in air and broadband calibration of microphones,” *J. Acoust. Soc. Am.* **137**(6), 3314–3324 (2015).
- <sup>3</sup>P. Lecomte, Q. Leclère, and S. Ollivier, “Equivalent source model from acousto-optic measurements and application to an acoustic pulse characterization,” *J. Sound Vib.* **450**, 141–155 (2019).
- <sup>4</sup>K. Ishikawa, Y. Shiraki, T. Moriya, A. Ishizawa, K. Hitachi, and K. Oguri, “Low-noise optical measurement of sound using midfringe locked interferometer with differential detection,” *J. Acoust. Soc. Am.* **150**(2), 1514–1523 (2021).
- <sup>5</sup>K. Bertling, J. Perchoux, T. Taimre, R. Malkin, D. Robert, A. D. Rakić, and T. Bosch, “Imaging of acoustic fields using optical feedback interferometry,” *Opt. Express* **22**(24), 30346 (2014).
- <sup>6</sup>P. F. Urgiles Ortiz, J. Perchoux, A. L. Arriaga, F. Jayat, and T. Bosch, “Visualization of an acoustic stationary wave by optical feedback interferometry,” *Opt. Eng.* **57**(05), 1 (2018).
- <sup>7</sup>K. Petermann, *Laser Diode Modulation and Noise* (Springer Netherlands, Dordrecht, 1988), pp. 250–290.
- <sup>8</sup>E. Knudsen, J. Perchoux, T. Mazoyer, F. Jayat, C. Tronche, and T. Bosch, “Lower detection limit of the acousto-optic effect using optical feedback interferometry,” in *2020 IEEE International Instrumentation and Measurement Technology Conference (I2MTC)*, Dubrovnik, Croatia (IEEE, Piscataway, NJ, 2020), pp. 1–4.
- <sup>9</sup>P. E. Ciddor, “Refractive index of air: New equations for the visible and near infrared,” *Appl. Opt.* **35**(9), 1566–1573 (1996).
- <sup>10</sup>R. Kliese, T. Taimre, A. A. A. Bakar, Y. L. Lim, K. Bertling, M. Nikolić, J. Perchoux, T. Bosch, and A. D. Rakić, “Solving self-mixing equations for arbitrary feedback levels: A concise algorithm,” *Appl. Opt.* **53**(17), 3723–3736 (2014).
- <sup>11</sup>C. Henry, “Theory of the linewidth of semiconductor lasers,” *IEEE J. Quantum Electron.* **18**(2), 259–264 (1982).
- <sup>12</sup>S. Donati, G. Giuliani, and S. Merlo, “Laser diode feedback interferometer for measurement of displacements without ambiguity,” *IEEE J. Quantum Electron.* **31**(1), 113–119 (1995).
- <sup>13</sup>D. Blackstock, *Fundamentals of Physical Acoustics* (Wiley, New York, 2000), pp. 421–424.